Diffusion-based Layer-wise Semantic Reconstruction for Unsupervised Out-of-Distribution Detection

Ying Yang^{1*}, De Cheng^{1*†}, Chaowei Fang^{1*†}, Yubiao Wang¹ Changzhe Jiao¹, Lechao Cheng², Nannan Wang¹, Xinbo Gao³

¹Xidian University

²Hefei University of Technology

³Chongqing University of Posts and Telecommunications
{yycfq, ybwang_3}@stu.xidian.edu.cn
chenglc@hfut.edu.cn, gaoxb@cqupt.edu.cn
{dcheng, cwfang, cjiao, nnwang}@xidian.edu.cn

Abstract

Unsupervised out-of-distribution (OOD) detection aims to identify out-of-domain data by learning only from unlabeled In-Distribution (ID) training samples, which is crucial for developing a safe real-world machine learning system. Current reconstruction-based method provides a good alternative approach, by measuring the reconstruction error between the input and its corresponding generative counterpart in the pixel/feature space. However, such generative methods face the key dilemma, i.e., improving the reconstruction power of the generative model, while keeping compact representation of the ID data. To address this issue, we propose the diffusion-based layer-wise semantic reconstruction approach for unsupervised OOD detection. The innovation of our approach is that we leverage the diffusion model's intrinsic data reconstruction ability to distinguish ID samples from OOD samples in the latent feature space. Moreover, to set up a comprehensive and discriminative feature representation, we devise a multi-layer semantic feature extraction strategy. Through distorting the extracted features with Gaussian noises and applying the diffusion model for feature reconstruction, the separation of ID and OOD samples is implemented according to the reconstruction errors. Extensive experimental results on multiple benchmarks built upon various datasets demonstrate that our method achieves state-of-the-art performance in terms of detection accuracy and speed. Code is available at https://github.com/xbyym/DLSR.

1 Introduction

Unsupervised Out-of-Distribution (OOD) detection aims to identify whether a data point belongs to the In-Distribution (ID) or OOD dataset, by learning only from unlabeled in-distribution training samples. OOD detection plays a vital role in developing a safe real-world machine learning system, which ensures that the model is only performed on data drawn from the same distribution as its training data. If the test data does not follow the training distribution, the model could unintentionally produce nonsensical predictions, resulting in some misleading conclusions. Naturally, OOD detection is one of the key techniques for ensuring the model's robustness and safety.

Existing research studies the OOD detection mainly under two settings, i.e., supervised and unsupervised. The supervised OOD detection methods usually deem this task as a binary classification problem, which relies on training with data labeled as OOD from disjoint categories or adversaries

38th Conference on Neural Information Processing Systems (NeurIPS 2024).

^{*} Equation Contribution. † Corresponding authors: De Cheng and Chaowei Fang.

[Hendrycks et al., 2018], [Ming et al., 2022]. However, in many practical applications, it is almost impossible to access representative OOD samples, as the OOD data usually can be highly diverse and unpredictable. Therefore, we prefer to study the more challenging while practical unsupervised OOD detection problem. We will build an OOD detector trained solely on unlabeled ID data, as large amounts of unlabeled data are readily available and widely utilized due to their ease of acquisition.

Current reconstruction-based methods provide a good alternative approach for OOD detection, by measuring the reconstruction error between the input and its corresponding generative counterpart in the pixel/feature space. Obviously, the generative models and metric learning evaluation strategies are the main research directions. However, such methods of the generative models always face the following key dilemma: The projected in-distribution latent feature space should be compressed sufficiently to capture the exclusive characteristics of ID images, while it should also provide sufficient reconstruction power for the large-scale ID images of various categories. Existing generative-based methods (e.g., auto-encoder (AE), variational AE [Kingma and Welling, 2013] and Generative Adversarial Network(GAN)) [Goodfellow et al., 2014], can not always fulfill these two requirements simultaneously, and a good balance between them is required. Besides, recent OOD detection methods based on diffusion models such as [Graham et al., 2023], [Gao et al., 2023] and [Liu et al., 2023] often involve the pixel-level reconstruction of distorted images, which consume much training/inference time and computation resources.

To address the above-mentioned issues, and inspired by the latent space noise addition mechanism in Latent Diffusion Models (LDM) Rombach et al. [2022], we propose the diffusion-based layerwise semantic reconstruction approach for unsupervised OOD detection. Specifically, the proposed method makes full use of the diffusion model's intrinsic data reconstruction ability, to distinguish in-distribution samples from OOD samples in the latent feature space. In the diffusion denoising probabilistic models (DDPM) [Ho et al., 2020], the model is trained to incrementally remove noise from the noised inputs of different levels. Clearly, we can see that, instead of faithfully reconstructing inputs from the distribution it was trained on as previous VAE Kingma and Welling [2013] or GAN Goodfellow et al. [2014], the diffusion-based model shows more powerful reconstruction capabilities. Practically, our model involves reconstructing an input image feature from multiple values of the time step, this allows a single trained model to handle large amount of noise applied to the input, obviating the need for any dataset-specific fine-tuning.

Moreover, to set up a comprehensive and discriminative feature representation, we devise a multilayer semantic feature extraction strategy. Performing feature reconstruction on top of the multi-layer semantic features, encourages to restrict the in-distribution latent features distributed more compactly within a certain space, so as to better rebuild in-distribution samples while not reconstructing OOD comparatively. Overall, by distorting the extracted multi-layer features with Gaussian noises and applying the diffusion model for feature reconstruction, the separation of ID and OOD samples is implemented according to the reconstruction errors. Note that, the proposed Latent Feature Diffusion Network (LFDN) is built on top of the feature level instead of the traditional pixel level, which could significantly improve the computation efficiency and achieve effective OOD detection. The other potential strength of such a strategy is that it avoids the reconstruction of minor characteristics unrelated to image understanding. In summary, the contributions of this work are as follows:

- We propose a diffusion-based layer-wise semantic reconstruction framework to tackle OOD
 detection, based on multi-layer semantic feature distortion and reconstruction. Meanwhile,
 We are the first to successfully incorporate generative modeling of features within the
 framework of OOD detection in image classification tasks.
- The layer-wise semantic feature reconstruction encourages restricting the in-distribution latent features to be more compactly distributed within a certain space, enabling better reconstruction of ID samples while limiting the reconstruction of OOD samples.
- Extensive experiments on multiple benchmarks across various datasets show that our method achieves state-of-the-art detection accuracy and speed.

2 Related Work

Existing researches study the OOD detection mainly under two settings: supervised and unsupervised. The Supervised method is generally based on classification. The method usually uses the maximum softmax probability [Hendrycks and Gimpel, 2016] from the final fully connected (FC) layer as the score to judge the ID sample. But the classification-based OOD detection methods often encounter

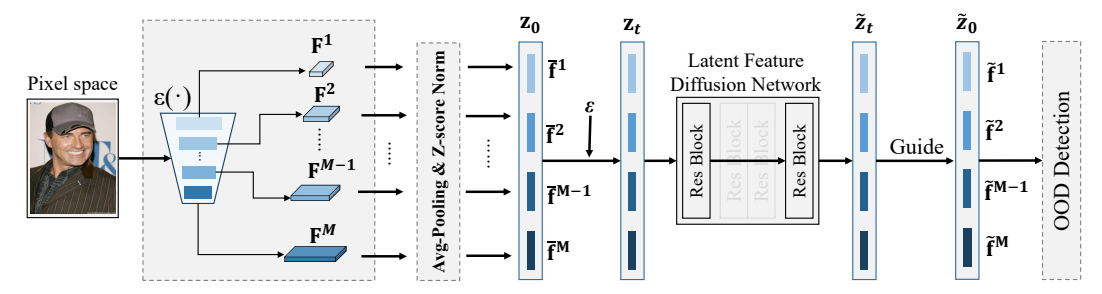


Figure 1: Overview of proposed diffusion-based layer-wise semantic reconstruction framework for unsupervised OOD detection. It includes multi-layer semantic feature extraction, Diffusion-based Feature Distortion and Reconstruction, and OOD detection head modules.

issues with assigning high softmax probability to OOD samples. Recent works [Liu et al., 2020], [Sun and Li, 2022], [Djurisic et al., 2022], [Zhao et al., 2024], attempt to alleviate this issue. The unsupervised OOD detection can be roughly categorized as the distance-based metric evaluation and the generative-based reconstruction methods.

Distance-based methods assume that OOD data lies far from ID class centroids. [Ren et al., 2021] improved OOD detection by separating image foregrounds from backgrounds and computing the Mahalanobis distance for each, then combining them. [Sun et al., 2022] used a non-parametric nearest neighbor distance for OOD detection. [Techapanurak et al., 2020] and [Chen et al., 2020] used cosine similarity to measure distances between test data features of in-distribution data to identify OOD data. [Huang et al., 2020] applied Euclidean distance, while [Gomes et al., 2022] used Geodesic distance for OOD detection. These methods often fail to capture sample distribution accurately.

Among the generative-based methods, the Likelihood-based methods can be traced back to as early as [Bishop, 1994]. This method assumes that the generative model assigns high likelihood to ID data, while the likelihood for OOD data tends to be lower. Recently, several deep generative models have supported the computation of likelihood, such as VAE [Kingma and Welling, 2013], PixelCNN++ [Salimans et al., 2017], and Glow [Kingma and Dhariwal, 2018]. However, some studies ([Nalisnick et al., 2018]; [Choi et al., 2018]; [Kirichenko et al., 2020]) have found that probabilistic generative models might also assign high likelihood to OOD data.

A series of studies have attempted to mitigate this issue. [Serrà et al., 2019] explored the relationship between image complexity and likelihood values, which adjusted likelihoods based on the size of image compression. [Ren et al., 2019] enhanced OOD detection by comparing likelihood values derived from different models. Another closely related approach highlights that these indicators are not well suited for VAEs. [Xiao et al., 2020] proposed a specialized metric known as likelihood regret for OOD detection in VAEs. [Cai and Li, 2023] suggested to leverage the high-frequency information of images to improve the model's ability to recognize OOD data. Additionally, a range of studies [Nalisnick et al., 2019], [Wang et al., 2020], [Bergamin et al., 2022], [Osada et al., 2023], have proposed typicality tests, estimating layer activation distributions and other statistical measures on training data, which are then evaluated through hypothesis testing or density estimation.

Another type of OOD detection methods leverage the idea that generative networks produce different reconstruction errors for ID and OOD data. Some methods such as [Sakurada and Yairi, 2014], [Zong et al., 2018], and [Zhou and Paffenroth, 2017], used auto-encoders to analyze reconstruction errors. GAN-based methods [Schlegl et al., 2017], [Zenati et al., 2018], and [Madzia-Madzou and Kuijf, 2022] utilized reconstruction errors and discriminator confidence to detect anomalies. Recent works [Graham et al., 2023], [Gao et al., 2023], and [Liu et al., 2023] applied diffusion models to model the pixel-level distribution of images, using errors from multiple reconstructions for OOD detection. Different from previous methods, we propose to leverage diffusion models to perform multi-layer semantic reconstruction in the latent feature space, not only for their stability in generation but also for significantly reducing training and inference time costs.

3 Method

Unsupervised OOD detection leverages intrinsic information from an unlabeled ID dataset \mathbb{D} to train a detector. Suppose \mathbb{D} contains N images, namely $\mathbb{D} = \{\mathbf{x}_i\}_{i=1}^N$, where \mathbf{x}_i denotes the i-th image.

The target is to learn an OOD detector denoted as $\mathcal{S}(\cdot)$, which can effectively evaluate an OOD score for each input image. The judgment of whether the input image belongs to ID or OOD is implemented by thresholding the OOD score. For example, given a testing image \mathbf{x} , it is recognized as an ID sample if the OOD score $\mathcal{S}(\mathbf{x})$ is lower than the pre-defined threshold λ ; otherwise, it is recognized as an OOD sample.

In this paper, we propose a diffusion-based layer-wise semantic reconstruction framework to accomplish the OOD detection task. Specifically, as illustrated in Figure 1, the proposed framework consists of the following three components: the multi-layer semantic feature extraction module, the latent feature diffusion stage, and the OOD detection head.

3.1 Multi-layer Semantic Feature Extraction

The proposed semantic reconstruction-based method achieves OOD detection by measuring the reconstruction error between the input and its generative counterpart in the feature space. Specifically, we devise a multi-layer semantic feature extraction strategy, to set up a comprehensive and discriminative feature representation for each input image. Such multi-layer features could better rebuild the samples and encourage the ID semantic features distributed more compactly within a certain space from different semantic layers.

Specifically, given an image $\mathbf{x} \in \mathbb{R}^{3 \times w \times h}$ with w and h being the width and height of the input image, passing through an image encoder $\mathcal{E}(\cdot)$, (e.g., EfficientNet[Tan and Le, 2019]), we can extract its feature maps from different layers (i.e., low-level) to high-level semantic blocks). The multi-layer intermediate feature map from the m-th block can be defined as $\mathbf{F}^m \in \mathbb{R}^{c_m \times w_m \times h_m}$, $m \in \{1,...,M\}$, where c_m , w_m and h_m are the number of channels, width and height of the feature map \mathbf{F}^m , and M is the total number of intermediate feature maps. Then, each feature map \mathbf{F}^m undergoes the global average pooling, obtaining the one-dimensional feature vector $\mathbf{f}^m \in \mathbb{R}^{c_m}$. Afterward, Z-score normalization [Al Shalabi et al., 2006] is applied to each feature vector \mathbf{f}^m , resulting in $\overline{\mathbf{f}}^m = \frac{\mathbf{f}^m - \mu_{\mathbf{f}^m}}{\sqrt{\mathrm{Var}(\mathbf{f}^m) + \delta}}$ for the m-th intermediate feature vector \mathbf{f}^m of the input image \mathbf{x} , where $\mathrm{Var}(\mathbf{f}^m)$ is the variance of \mathbf{f}^m along the channel elements, and δ is a small constant value. Finally, we obtain the overall multi-layer feature vector for the input image \mathbf{x} as: $\mathbf{z}_0 = \mathcal{H}(\mathbf{x}) = [\overline{\mathbf{f}}^1, \ldots, \overline{\mathbf{f}}^m, \ldots, \overline{\mathbf{f}}^M] \in \mathbb{R}^c$ by concatenating all the intermediate feature vectors, where $c = \sum_{m=1}^M c_m$, and $\mathcal{H}(\mathbf{x})$ denotes the whole feature extraction process.

3.2 Diffusion-based Feature Distortion and Reconstruction

Fitting the semantic feature distribution of ID samples is crucial for identifying whether the input is an ID or OOD sample. However, it is difficult to explicitly model the semantic feature space which has moderate complexity. Existing generative-based models [Zhou, 2022], [Cai and Li, 2023] address the modeling of complex data/feature space by transferring the original data/features into an implicit bottleneck space and learning a generator capable of recovering ID samples from the bottleneck space. Since the generator can not generalize well in recovering unseen OOD samples, it can be used as the OOD detector. Inspired by this, we set up a diffusion-based feature distortion and reconstruction framework, considering

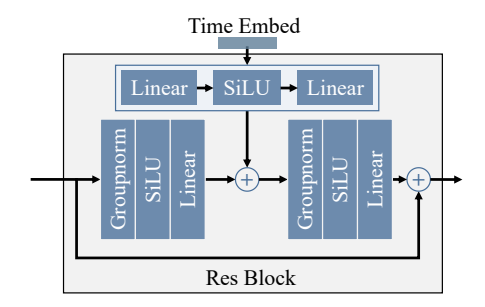


Figure 2: Residual Block Structure in LFDN.

the strength of diffusion models in data reconstruction. Our framework is innovative in the introduction of diffusion models in modeling semantic features, while previous works [Graham et al., 2023], [Liu et al., 2023], [Gao et al., 2023] focus on applying diffusion models for straightforward pixel-level distortion and reconstruction.

Semantic Feature Distortion.

The semantic feature distortion process can be conceptualized as transforming the semantic features into distorted counterparts with different levels of noise. For each step t belonging to $[1, \ldots, T]$, the

generation of data point \mathbf{z}_t follows the formula:

$$\mathbf{z}_t = \text{ennoise}(\mathbf{z}_0, t) = \sqrt{\overline{\alpha}_t} \times \mathbf{z}_0 + \sqrt{1 - \overline{\alpha}_t} \times \boldsymbol{\epsilon}, \quad \boldsymbol{\epsilon} \sim \mathcal{N}(\mathbf{0}^c, \mathbf{I}^{c \times c})$$
 (1)

where $\epsilon \in \mathbb{R}^c$ represents a Gaussian noise vector; $\mathcal{N}(\cdot, \cdot)$ denotes the Gaussian distribution; $\mathbf{0}^c$ and $\mathbf{I}^{c \times c}$ denote the c-dimensional zero vector and the $c \times c$ identity matrix, respectively. $\overline{\alpha}_t$ is a predefined noise level that controls the amount of noise added at each step.

Semantic Feature Reconstruction. For reconstructing the semantic features from their distorted counterparts, we build up a Latent Feature Diffusion Network (LFDN) constituted by 16 residual blocks (ResBlock), as shown in Fig. 1.

The structure of ResBlock is illustrated in Fig. 2. Its residual branch is formed with two groups of Groupnorm [Wu and He, 2018], SiLU, and linear layers, as well as a MLP used for absorbing in the time embedding.

Following the calculation process of the denoising diffusion implicit model [Song et al., 2020], we employ LFDN to remove the noises injected into the semantic features with skipping step stride denoted as s. The detailed noise-removing process for \mathbf{z}_t is described as follows. s is set to a value randomly selected from $\{1, 2, \cdots, t\}$.

- 1) We first input \mathbf{z}_t and the time embedding of t into LFDN, generating an initial reconstruction state denoted as $\tilde{\mathbf{z}}_t$. The calculation formulation can be summarized as: $\tilde{\mathbf{z}}_t = \text{LFDN}(\mathbf{z}_t, t)$, where LFDN(·) denotes the feed-forward process of LFDN.
- 2) Afterwards, we estimate the noise correction vector for \mathbf{z}_t denoted as $\tilde{\boldsymbol{\epsilon}}_t$ as follows,

$$\tilde{\boldsymbol{\epsilon}}_t = \frac{\mathbf{z}_t - \sqrt{\overline{\alpha}_t} \times \tilde{\mathbf{z}}_t}{\sqrt{1 - \overline{\alpha}_t}},\tag{2}$$

where $\overline{\alpha}_t$ is the predefined noise level of the t-th feature distortion step.

3) Then, we sample the input $(\tilde{\mathbf{z}}_{t'})$ for implementing the t'-th step's feature reconstruction where $t' = \max(t - s, 0)$ as:

$$\tilde{\mathbf{z}}_{t'} = \sqrt{\overline{\alpha}_{t'}} \left(\frac{\mathbf{z}_t - \sqrt{1 - \overline{\alpha}_t} \times \tilde{\boldsymbol{\epsilon}}_t)}{\sqrt{\overline{\alpha}_t}} + \sqrt{1 - \overline{\alpha}_{t'} - \sigma_t^2} \times \tilde{\boldsymbol{\epsilon}}_t \right) + \sigma_t^2 \boldsymbol{\epsilon}, \tag{3}$$

where σ_t^2 represents the variance of the additional noise at step t. Regarding $\tilde{\mathbf{z}}_{t'}$ and time embedding of t' as inputs, LFDN predicts reconstruction results of the t'-th step as $\tilde{\mathbf{z}}_{t'} = \text{LFDN}(\tilde{\mathbf{z}}_{t'}, t')$.

4) Repeating steps 2 and 3 until t' = 0, yields the final reconstructed semantic features $\tilde{\mathbf{z}}_0$.

We summarize the above process as $\tilde{\mathbf{z}}_0 = \text{denoise}(\mathbf{z}_t, t)$. This framework ensures that $\tilde{\mathbf{z}}_0$ is not solely derived from the LFDN output but is continuously refined by DDIM, integrating detailed corrections to achieve high accuracy in reconstructing the original data from its noisy observations.

Objective Function. For optimizing the network parameters of LFDN, the mean square error is used as the loss function for pulling close the outputs of LFDN with the original semantic features. The calculation formulation is as follows:

$$L = \frac{1}{N} \sum_{\mathbf{x} \in \mathbb{D}} \|\mathbf{z}_0 - \text{LFDN}(\mathbf{z}_t, t)\|_2^2$$
(4)

During training, t is randomly selected from $\{1, 2, \dots, T\}$. The detail is illustrated in Algorithm 1.

3.3 OOD Detection Head

Our approach can be integrated with three metrics to detect OOD data. Firstly, we utilize the Mean Squared Error (MSE) to measure the feature reconstruction error. Secondly, we use the Likelihood Regret metric (LR = $MSE_{initial} - MSE_{final}$) [Xiao et al., 2020], which quantifies the change in MSE from the initial epoch to the final epoch. This metric reflects the model's evolving certainty during training. Generally, the reconstruction errors for ID samples decrease as the model becomes more familiar with these samples, whereas the errors for OOD samples remain relatively stable.

Lastly, we employ the Multi-layer Semantic Feature Similarity (MFsim), *i.e.*, the cosine similarity. We assesses the cosine similarity between the original features $\mathbf{z}_0 = [\overline{\mathbf{f}}^1, \dots, \overline{\mathbf{f}}^M, \dots, \overline{\mathbf{f}}^M]$ and the reconstructed features $\tilde{\mathbf{z}}_0 = [\tilde{\mathbf{f}}^1, \dots, \tilde{\mathbf{f}}^m, \dots, \tilde{\mathbf{f}}^M]$ at various layers: $\mathrm{Sim}(\overline{\mathbf{f}}^m, \tilde{\mathbf{f}}^m) = \frac{\overline{\mathbf{f}}^m.\tilde{\mathbf{f}}^m}{\|\overline{\mathbf{f}}^m\|.\|\overline{\mathbf{f}}^m\|}$. The OOD detection score MFsim, is then computed as the negative average of these similarities: MFsim = $-\frac{1}{M}\sum_{m=1}^M \mathrm{Sim}(\overline{\mathbf{f}}^m, \tilde{\mathbf{f}}^m)$, where M is the number of feature maps. A higher MFsim score indicates a greater likelihood of the data being OOD. Algorithm 2 details the MFsim calculation. The flows for MSE and LR calculations are provided in Appendix A.

Algorithm 1 Training Algorithm

```
1: Input: Train image \mathbf{x} \in \mathbb{R}^{3 \times h \times w}
2: \mathbf{z}_0 = \mathcal{H}(\mathbf{x}) = [\overline{\mathbf{f}}^1, \dots, \overline{\mathbf{f}}^m, \dots, \overline{\mathbf{f}}^M] \in \mathbb{R}^c
3: repeat
4: Draw t \sim \text{Uniform}\{1, \dots, T\}
5: Draw \epsilon \sim \mathcal{N}(0, I)
6: Compute \mathbf{z}_t and L
7: \mathbf{z}_t = \sqrt{\overline{\alpha}_t} \mathbf{z}_0 + \sqrt{1 - \overline{\alpha}_t} \epsilon
8: L = \frac{1}{N} \sum_{\mathbf{x} \in \mathbb{D}} \|\mathbf{z}_0 - \text{LFDN}(\mathbf{z}_t, t)\|_2^2
9: Update the parameters via the AdamW optimizer.
10: until convergence
```

Algorithm 2 Testing Algorithm

```
1: Input: An image \mathbf{x} \in \mathbb{R}^{3 \times h \times w}

2: Output: OOD score

3: \mathbf{z}_0 = \mathcal{H}(\mathbf{x}) = [\overline{\mathbf{f}}^1, \dots, \overline{\mathbf{f}}^m, \dots, \overline{\mathbf{f}}^M] \in \mathbb{R}^c

4: \mathbf{z}_t \leftarrow \text{ennoise}(\mathbf{z}_0, t)

5: \tilde{\mathbf{z}}_0 \leftarrow \text{denoise}(\mathbf{z}_t, t)

6: [\tilde{\mathbf{f}}^1, \dots, \tilde{\mathbf{f}}^m, \dots, \tilde{\mathbf{f}}^M] \leftarrow \tilde{\mathbf{z}}_0

7: for m = 1 to M do

8: S_m \leftarrow \text{Sim}(\overline{\mathbf{f}}^m, \tilde{\mathbf{f}}^m)

9: end for

10: MFsim \leftarrow -\left(\sum_{m=1}^M S_m\right)/M

11: return MFsim
```

4 Experiments

4.1 Datasets and Evaluation Metrics

Datasets: We train the OOD detection model on three in-distribution (ID) datasets: CIFAR-10 [Krizhevsky et al., 2009], CIFAR-100, and CelebA [Liu et al., 2015]. When testing models learned on a specific ID dataset, we select several datasets from SVHN [Netzer et al., 2011], SUN [Xiao et al., 2010], LSUN-c [Yu et al., 2015], LSUN-r, iSUN [Xu et al., 2015], iNaturalist [Van Horn et al., 2018], Textures [Cimpoi et al., 2014], Places365 [Zhou et al., 2017], MNIST [Deng, 2012], FMNIST, KMNIST [Clanuwat et al., 2018], Omniglot [Lake et al., 2015], and NotMNIST as OOD data.

Evaluation Metrics: We employed the area under the receiver operating characteristic (AUROC) and the false positive rate at 95% true positive rate (FPR95) as evaluation metrics. Results in FPR95 metric are provided in Appendix C.1.

4.2 Implementation Details

We utilize EfficientNet-b4 [Tan and Le, 2019] or ResNet50 [He et al., 2016] pre-trained on ImageNet [Deng et al., 2009] as our encoder. The main text presents results using EfficientNet-b4, while results using ResNet50 are detailed in Appendix C.2. For EfficientNet-b4, we select feature maps from the first to fifth stages (M=5) to construct the multi-layer semantic features, resulting in a feature dimension (c) of 720. The LFDN is consisting of 16 residual blocks. Inside each residual block, the number of groups in Groupnorm and the intermediate feature dimension of the residual branch are set to 1 and 1440, respectively. We employ the AdamW optimizer with a weight decay of 10^{-4} . Our method is trained on NVIDIA Geforce 4090 GPU for 150 epochs, with a batch size of 128 and a constant learning rate of 10^{-4} throughout the training phase.

4.3 Comparison with State-of-the-art Methods

Compared Generative-based Methods: In Table 1, regarding CIFAR-10 as the ID dataset, we compare our method against pixel-level generative-based methods including GLOW [Serrà et al., 2019], PixelCNN++ [Serrà et al., 2019], VAE [Xiao et al., 2020], and DDPM [Graham et al., 2023]. To validate the effectiveness of LFDN, we implement a variant of our method through replacing LFDN with AutoEncoder in which MFsim is used for estimating the OOD score. In comparison with the best

pixel-level method, VAE, our method achieves a 9.1% improvement in average AUROC when using MFsim for OOD score estimation. Compared to DDPM, our method variants show a significantly improvement in average AUROC. For example, when integrated with MSE, our method achieves 20.4% higher AUROC than DDPM. This indirectly indicates that performing OOD detection at the pixel level is much worse than performing OOD detection at the feature level. Generating pixels may reconstruct more content unrelated to the image's semantics, which may interfere the identification of OOD samples. Making the model focus on the reconstruction of compactly distributed semantic features benefits in separating ID and OOD samples. In terms of testing speed, our method is nearly 100 times faster than DDPM, significantly enhancing performance while reducing detection costs. Moreover, the final version of our method built upon LFDN improves average AUROC by 18.5% compared to the variant basd on AutoEncoder, as the diffusion model captures data distribution more effectively.

In Table 2, we compare our method with VAE, DDPM and AutoEncoder, using CelebA as the ID dataset. Our method integrated with MFsim achieves state-of-the-art performances, with an AUROC improvement of 19.89% compared to DDPM, and the performance of the remaining two metrics also far exceeds the baseline, demonstrating the generalizability of our approach.

Compared Classification-based and Distance-based Methods: In Table 3, we compare our method with classification-based methods including MSP [Hendrycks and Gimpel, 2016], EBO [Liu et al., 2020], DICE [Sun and Li, 2022], and ASH-S [Djurisic et al., 2022], as well as distance-based methods including 'SimCLR+Mahalanobis Distance' [Xiao et al., 2021] and 'SimCLR+KNN' [Sun et al., 2022]. All methods are evaluated using EfficientNet-b4 as the backbone. Compared to classification-based and distance-based methods, our approach consistently shows a clear advantage. Specifically, for CIFAR-100 as the in-distribution dataset, our method integrated with MFsim achieves an average AUROC of 13.84% higher than the classification-based method DICE. Moreover, unlike classification-based methods, our approach does not require labeled data.

The inference speed of our method based on MSE or MFsim is faster than that of distance-based methods SimCLR+Maha and SimCLR+KNN, because the computation of covariance matrix or K nearest neighbors occupies part of time. Our method is also comparable to classifier-based methods including MSP, EBO, DICE and ASH-S. This demonstrates the effectiveness of leveraging the strong ability of diffusion models to reconstruct original distributions from different noise levels for reconstructing low-dimensional features and performing OOD detection.

Table 1: The AUROC values for OOD detection, where CIFAR-10 is used as the in-distribution dataset. The results are compared with generative-based methods. Higher AUROC values indicate better performance, with the best results highlighted in bold for clarity.

D	ataset		Pixel-Generativ	ve-Base			Feature-Ger	erative-Base	
ID	OOD	GLOW	PixelCNN++	VAE	DDPM	AutoEncoder	our(+MSE)	ours(+LR)	ours(+MFsim)
	SVHN	88.3	73.7	95.9	97.3	57.7	97.3±0.0	98.2±0.0	98.9±0.1
	LSUN	21.3	64.0	40.3	68.2	81.5	97.6 ± 0.1	97.8 ± 0.1	99.8 \pm 0.1
	MNIST	85.8	96.7	99.9	83.2	95.8	99.4 ± 0.0	98.9 ± 0.1	99.9 \pm 0.0
CIFRA10	FMNIST	71.2	90.7	99.1	84.3	79.6	99.0 ± 0.0	98.8 ± 0.0	99.9 \pm 0.0
CHRITO	KMNIST	38.0	82.6	99.9	89.7	90.5	99.5 ± 0.0	99.1 ± 0.0	99.9 ± 0.0
	Omniglot	95.5	98.9	99.6	35.9	81.5	99.1 ± 0.1	97.1 ± 0.1	99.9 ± 0.0
	NotMNIST	53.9	82.6	99.4	88.7	81.6	99.8 ± 0.1	99.5 ± 0.0	99.9 \pm 0.0
	average	64.9	84.2	90.6	78.2	81.2	98.8±0.1	98.5±0.1	99.7±0.1
Time	Num img/s (†)	38.6	19.3	0.7	11.4	1224.2	999.3	273.6	999.3

4.4 Ablation Study

Illustration of the generation ability of the diffusion model on OOD detection. To demonstrate the evolution of the generative model's reconstruction capability for both ID and OOD samples before and after training, we compare the distributions of the MFsim scores at the first epoch and the final epoch in Figure 3. CIFAR-10 serves as the ID dataset, while the other six datasets listed in Table 3 are employed as OOD data. Our observations reveal that the diffusion model's reconstruction ability enhances across most datasets, with a notably more pronounced improvement for the in-distribution samples. This indicates that ID samples are reconstructed more effectively, thereby validating the efficacy of our method.

Table 2: The AUROC values for OOD detection, where CelebA is used as the in-distribution dataset. The results are compared with generative-based methods. Higher AUROC values indicate better performance, with the best results highlighted in bold for clarity.

	Dataset	Pixel-C	Generative-Based		Feature-Gen	Feature-Generative-Based			
ID	OOD	VAE	DDPM	AutoEncoder	ours(+MSE)	ours(+LR)	ours(+MFsim)		
	SUN	95.89	83.41	32.90	99.98±0.01	97.15±0.02	99.98±0.01		
	iNaturalist	95.52	82.38	41.56	100+0.00	99.96 ± 0.01	99.99 ± 0.00		
CelebA	Textures	91.73	78.33	56.33	99.93 ± 0.02	98.51 ± 0.02	99.96 ± 0.01		
	Places365	97.58	76.25	35.90	99.96 ± 0.01	97.47 ± 0.03	99.98 ± 0.00		
	average	95.18	80.09	41.67	99.97 ± 0.01	98.27 ± 0.02	99.98±0.01		
Time	Num img/s (†)	18.7	10.2	1357.6	1033.8	290.4	1033.8		

Table 3: The AUROC values for OOD detection, where CIFAR-10/100 is used as the in-distribution dataset. The results are compared with Classification-based and Distance-based methods using EfficientNet-b4 as the backbone. Higher AUROC values indicate better performance, with the best results highlighted in bold for clarity.

	<u> </u>					O	OD			
ID	Based	Method	Num img/s (†)	SVHN	LSUN-c	LSUN-r	iSUN	Textures	Places365	average
		MSP	1060.5	94.53	96.37	91.80	92.23	95.93	97.59	94.74
	l	EBO	1060.5	96.79	97.34	94.42	94.64	96.30	98.34	96.31
	Classifier-based	DICE	1066.3	98.53	99.03	94.49	95.25	97.68	99.63	97.44
		ASH-S	1047.6	98.01	98.23	93.17	94.13	97.01	98.48	96.51
CIFAR10		SimCLR+Mahalanobis	674.8	97.80	73.61	69.28	88.63	76.47	67.42	78.87
CHARTO	Distance-based	SimCLR+KNN	919.8	92.40	92.05	89.81	90.14	97.24	94.36	92.67
	Generative-based	ours(+MSE)	960.6	97.31±0.02	97.59 ± 0.01	93.93±0.01	92.78 ± 0.01	$100 {\pm} 0.00$	99.96±0.00	96.93±0.01
		ours(+LR)	360.2	98.22±0.02	97.84 ± 0.02	95.37 ± 0.01	94.31 ± 0.02	100 ± 0.00	99.91 ± 0.01	97.61±0.02
		ours(+MFsim)	960.6	98.89±0.01	99.83 \pm 0.02	98.83 ± 0.01	98.52 ± 0.02	$100 {\pm} 0.00$	$100 {\pm} 0.00$	99.34±0.01
		MSP	1060.5	77.56	84.03	72.09	71.52	90.02	89.00	80.70
		EBO	1060.5	76.51	81.59	78.92	76.38	79.38	83.07	79.31
	Classifier-based	DICE	1066.3	86.93	88.54	71.97	71.29	92.83	90.78	83.72
		ASH-S	1047.6	92.11	90.03	63.30	65.12	95.25	92.99	83.13
CIFAR100		SimCLR+Mahalanobis	674.8	56.24	52.23	61.34	73.53	71.92	51.98	61.21
CHIMCIOO	Distance-based	SimCLR+KNN	919.8	54.37	51.49	83.80	77.21	53.31	54.43	62.44
		ours(+MSE)	960.6	83.93±0.01	86.86 ± 0.01	75.38 ± 0.01	71.99 ± 0.02	99.99 ± 0.00	99.97±0.01	86.35±0.01
	Generative-based	ours(+LR)	360.2	88.84±0.01	87.60 ± 0.02	80.96 ± 0.01	77.71 ± 0.02	99.98 ± 0.01	99.92 ± 0.02	89.17±0.01
		ours(+MFsim)	960.6	93.90±0.01	99.14 \pm 0.01	95.74 ± 0.01	94.40 ± 0.01	100 ± 0.00	100 ± 0.00	97.20±0.01

Performance variations across different sampling time steps: Figure 4 illustrates the variations in average AUROC and FPR95 values for different evaluation metrics at various sampling time steps, using CIFAR-10 as the ID data, with the final time step T=100. It is observed that all metrics perform poorly at t=1 primarily due to minimal noise added, making \mathbf{z}_t too similar to \mathbf{z}_0 and thus, limiting the denoising capability of LFDN; both ID and OOD data are well reconstructed. As t increases to about 3-10 steps, the appropriate amount of noise allows MSE, LR, and MFsim to reach optimal performances. However, as t continues to increase, the difference between \mathbf{z}_t and the original \mathbf{z}_0 enlarges, with \mathbf{z}_t gradually approaching random noise, thereby worsening the reconstruction differences between $\tilde{\mathbf{z}}_0$ and \mathbf{z}_0 for both ID and OOD samples.

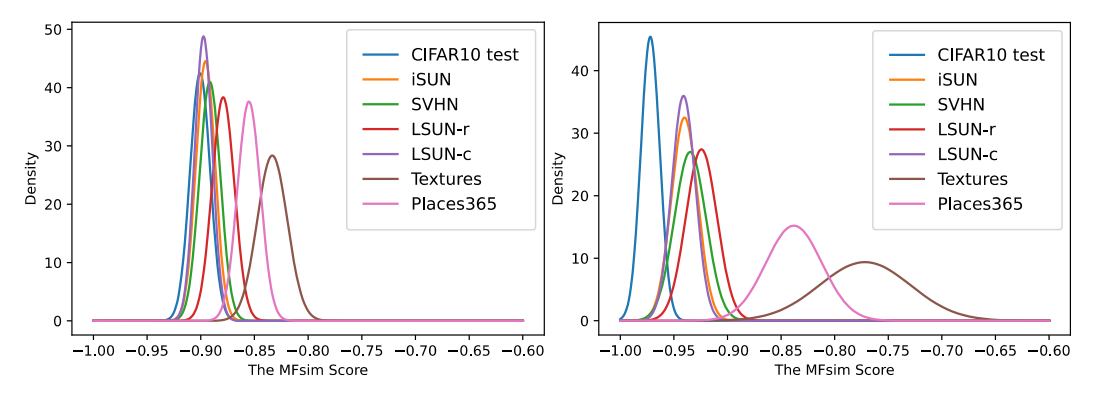
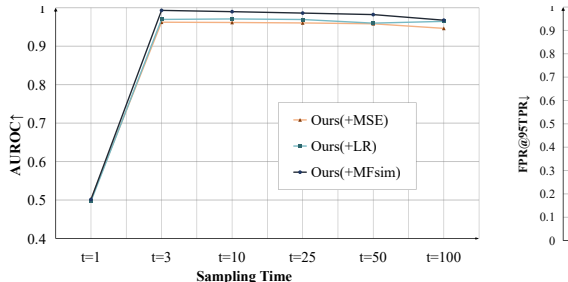


Figure 3: The MFsim score distributions of the first epoch (left) and the last epoch (right)



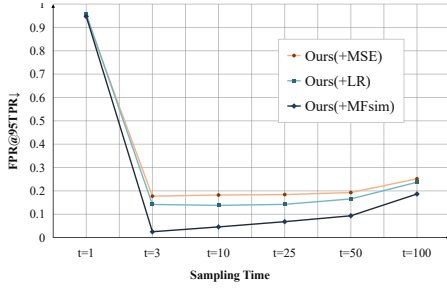


Figure 4: CIFAR-10 dataset is the ID data, the six datasets listed in Table 3 are used as OOD data. The average AUROC and FPR95 for the three metrics are evaluated at different sampling time steps.

Table 4: Changes in Average AUROC Across Six Datasets listed in Table 3 for CIFAR100 as ID.

Metrics	M	ISE	I	LR.	MFsim		
Linear	Linear=720	Linear=1440	Linear=720	Linear=1440	Linear=720	Linear=1440	
Average	83.35	86.35	84.05	89.17	96.43	97.20	
Number of Blocks	Number=8	Number=16	Number=8	Number=16	Number=8	Number=16	
Average	85.26	86.35	87.32	89.17	97.13	97.20	

Comparison of MFsim across different feature scales. Figure 5 displays performance comparisons of MFsim when reconstructing the last block (i.e., f_4 , C=448) versus multi-layer semantic features under an EfficientNet-b4 encoder. The results demonstrate that multi-layer semantic features generally outperform single-layer ones, indicating that multi-layer semantic features contain richer semantic information and are more representative of samples across different in-distribution datasets. Furthermore, considering the diverse semantic information represented by different layers, combing various layers of semantic features helps to boost the OOD performances of LFDN.

Ablation study on LFDN network parameters. We conducted ablation experiments on two groups of parameters within the LFDN network: the dimension of the linear layers and the number of ResBlocks. For each experiment, we reduced one of these parameters to half of its original size while keeping all other parameters unchanged. **Table 4** presents the results of these experiments, showing how these modifications affect the performance. It is observed that the performance of our MFsim metric remains relatively stable, indicating that it continues to provide effective OOD detection capabilities even under conditions of reduced network size.

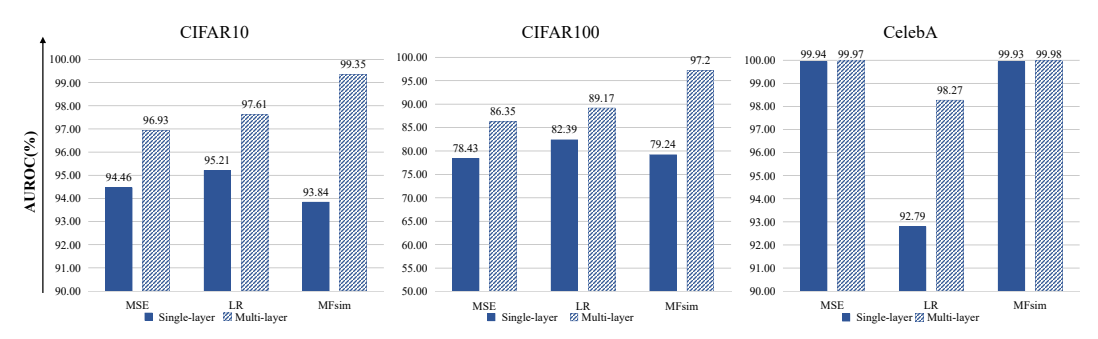


Figure 5: Variation of Average AUROC Values across Different Scales

5 Conclusion and Limitation

In this paper, we propose a diffusion-based layer-wise semantic reconstruction framework for unsupervised OOD detection. We leverage the diffusion model's intrinsic data reconstruction ability to distinguish in-distribution and OOD samples in the latent feature space. Specially, the diffusion-based feature generation is built on top of the devised multi-layer semantic feature extraction strategy, which

sets up a comprehensive and discriminative feature representation benefiting the generative OOD detection methods. Finally, we hope our proposed OOD detection method could make contributions to develop a safe real-world machine learning system. Additionally, it needs to point out that the performance of our method also relies on the quality of features extracted by the encoder. Therefore, selecting an encoder with strong feature extraction capabilities is crucial for achieving good performances.

6 Acknowledgement

This work was supported in part by the National Key R&D Program of China under Grant No.2023YFA1008600, in part by NSFC under Grant NO.62376206, 62176198 and U22A2096, in part by the Key R&D Program of Shaanxi Province under Grant 2024GX-YBXM-135, in part by the Key Laboratory of Big Data Intelligent Computing under Grant BDIC-2023-A-004.

7 Broader Impacts

Positive Societal Impacts: The proposed diffusion-based layer-wise semantic reconstruction method for unsupervised out-of-distribution (OOD) detection can significantly enhance the security and safety of machine learning systems. By effectively identifying OOD data, the system can prevent incorrect or potentially harmful decisions, making AI applications more reliable in critical areas such as healthcare, autonomous driving, and financial systems. This method increases the robustness of AI systems by ensuring they can handle unexpected inputs gracefully. This contributes to the overall stability and trustworthiness of AI deployments in various industries, thereby promoting wider acceptance and integration of AI technologies. Negative Societal Impacts: As with any advanced detection method, there is a risk that the technology could be misused. For instance, surveillance applications, it could be employed to monitor individuals without their consent, leading to privacy violations and ethical concerns.

References

- Dan Hendrycks, Mantas Mazeika, and Thomas Dietterich. Deep anomaly detection with outlier exposure. *arXiv preprint arXiv:1812.04606*, 2018.
- Yifei Ming, Ying Fan, and Yixuan Li. Poem: Out-of-distribution detection with posterior sampling. In *International Conference on Machine Learning*, pages 15650–15665. PMLR, 2022.
- Diederik P Kingma and Max Welling. Auto-encoding variational bayes. *arXiv preprint* arXiv:1312.6114, 2013.
- Ian Goodfellow, Jean Pouget-Abadie, Mehdi Mirza, Bing Xu, David Warde-Farley, Sherjil Ozair, Aaron Courville, and Yoshua Bengio. Generative adversarial nets. In Z. Ghahramani, M. Welling, C. Cortes, N. Lawrence, and K.Q. Weinberger, editors, *Advances in Neural Information Processing Systems*, volume 27. Curran Associates, Inc., 2014. URL https://proceedings.neurips.cc/paper_files/paper/2014/file/5ca3e9b122f61f8f06494c97b1afccf3-Paper.pdf.
- Mark S Graham, Walter HL Pinaya, Petru-Daniel Tudosiu, Parashkev Nachev, Sebastien Ourselin, and Jorge Cardoso. Denoising diffusion models for out-of-distribution detection. In *Proceedings of the IEEE/CVF Conference on Computer Vision and Pattern Recognition*, pages 2947–2956, 2023.
- Ruiyuan Gao, Chenchen Zhao, Lanqing Hong, and Qiang Xu. Diffguard: Semantic mismatch-guided out-of-distribution detection using pre-trained diffusion models. In *Proceedings of the IEEE/CVF International Conference on Computer Vision*, pages 1579–1589, 2023.
- Zhenzhen Liu, Jin Peng Zhou, Yufan Wang, and Kilian Q Weinberger. Unsupervised out-of-distribution detection with diffusion inpainting. In *International Conference on Machine Learning*, pages 22528–22538. PMLR, 2023.
- Robin Rombach, Andreas Blattmann, Dominik Lorenz, Patrick Esser, and Björn Ommer. High-resolution image synthesis with latent diffusion models. In *Proceedings of the IEEE/CVF conference on computer vision and pattern recognition*, pages 10684–10695, 2022.

- Jonathan Ho, Ajay Jain, and Pieter Abbeel. Denoising diffusion probabilistic models. *Advances in neural information processing systems*, 33:6840–6851, 2020.
- Dan Hendrycks and Kevin Gimpel. A baseline for detecting misclassified and out-of-distribution examples in neural networks. *arXiv preprint arXiv:1610.02136*, 2016.
- Weitang Liu, Xiaoyun Wang, John Owens, and Yixuan Li. Energy-based out-of-distribution detection. *Advances in neural information processing systems*, 33:21464–21475, 2020.
- Yiyou Sun and Yixuan Li. Dice: Leveraging sparsification for out-of-distribution detection. In *European Conference on Computer Vision*, pages 691–708. Springer, 2022.
- Andrija Djurisic, Nebojsa Bozanic, Arjun Ashok, and Rosanne Liu. Extremely simple activation shaping for out-of-distribution detection. *arXiv preprint arXiv:2209.09858*, 2022.
- Qinyu Zhao, Ming Xu, Kartik Gupta, Akshay Asthana, Liang Zheng, and Stephen Gould. Towards optimal feature-shaping methods for out-of-distribution detection. *arXiv preprint arXiv:2402.00865*, 2024.
- Jie Ren, Stanislav Fort, Jeremiah Liu, Abhijit Guha Roy, Shreyas Padhy, and Balaji Lakshminarayanan. A simple fix to mahalanobis distance for improving near-ood detection. *arXiv preprint arXiv:2106.09022*, 2021.
- Yiyou Sun, Yifei Ming, Xiaojin Zhu, and Yixuan Li. Out-of-distribution detection with deep nearest neighbors. In *International Conference on Machine Learning*, pages 20827–20840. PMLR, 2022.
- Engkarat Techapanurak, Masanori Suganuma, and Takayuki Okatani. Hyperparameter-free out-of-distribution detection using cosine similarity. In *Proceedings of the Asian conference on computer vision*, 2020.
- Xingyu Chen, Xuguang Lan, Fuchun Sun, and Nanning Zheng. A boundary based out-of-distribution classifier for generalized zero-shot learning. In *European conference on computer vision*, pages 572–588. Springer, 2020.
- Haiwen Huang, Zhihan Li, Lulu Wang, Sishuo Chen, Bin Dong, and Xinyu Zhou. Feature space singularity for out-of-distribution detection. *arXiv preprint arXiv:2011.14654*, 2020.
- Eduardo Dadalto Camara Gomes, Florence Alberge, Pierre Duhamel, and Pablo Piantanida. Igeood: An information geometry approach to out-of-distribution detection. *arXiv* preprint arXiv:2203.07798, 2022.
- Christopher M Bishop. Novelty detection and neural network validation. *IEE Proceedings-Vision*, *Image and Signal processing*, 141(4):217–222, 1994.
- Tim Salimans, Andrej Karpathy, Xi Chen, and Diederik P Kingma. Pixelcnn++: Improving the pixelcnn with discretized logistic mixture likelihood and other modifications. *arXiv* preprint *arXiv*:1701.05517, 2017.
- Durk P Kingma and Prafulla Dhariwal. Glow: Generative flow with invertible 1x1 convolutions. *Advances in neural information processing systems*, 31, 2018.
- Eric Nalisnick, Akihiro Matsukawa, Yee Whye Teh, Dilan Gorur, and Balaji Lakshminarayanan. Do deep generative models know what they don't know? *arXiv preprint arXiv:1810.09136*, 2018.
- Hyunsun Choi, Eric Jang, and Alexander A Alemi. Waic, but why? generative ensembles for robust anomaly detection. *arXiv preprint arXiv:1810.01392*, 2018.
- Polina Kirichenko, Pavel Izmailov, and Andrew G Wilson. Why normalizing flows fail to detect out-of-distribution data. *Advances in neural information processing systems*, 33:20578–20589, 2020.
- Joan Serrà, David Álvarez, Vicenç Gómez, Gregory Slabaugh, and Isabel Diez. Input complexity and out-of-distribution detection with likelihood-based generative models. *Proceedings of the International Conference on Learning Representations*, 2019.

- Jie Ren, Peter J. Liu, Emily Fertig, Jasper Snoek, Ryan Poplin, Mark DePristo, Joshua Dillon, and Balaji Lakshminarayanan. Likelihood ratios for out-of-distribution detection. *Advances in Neural Information Processing Systems*, 32, 2019.
- Zhisheng Xiao, Qing Yan, and Yali Amit. Likelihood regret: An out-of-distribution detection score for variational auto-encoder. *Advances in neural information processing systems*, 33:20685–20696, 2020.
- Mu Cai and Yixuan Li. Out-of-distribution detection via frequency-regularized generative models. In *Proceedings of the IEEE/CVF Winter Conference on Applications of Computer Vision*, pages 5521–5530, 2023.
- Eric Nalisnick, Akihiro Matsukawa, Yee Whye Teh, and Balaji Lakshminarayanan. Detecting out-of-distribution inputs to deep generative models using typicality. *arXiv preprint arXiv:1906.02994*, 2019
- Ziyu Wang, Bin Dai, David Wipf, and Jun Zhu. Further analysis of outlier detection with deep generative models. *Advances in Neural Information Processing Systems*, 33:8982–8992, 2020.
- Federico Bergamin, Pierre-Alexandre Mattei, Jakob Drachmann Havtorn, Hugo Senetaire, Hugo Schmutz, Lars Maaløe, Soren Hauberg, and Jes Frellsen. Model-agnostic out-of-distribution detection using combined statistical tests. In *International Conference on Artificial Intelligence and Statistics*, pages 10753–10776. PMLR, 2022.
- Genki Osada, Tsubasa Takahashi, Budrul Ahsan, and Takashi Nishide. Out-of-distribution detection with reconstruction error and typicality-based penalty. In *Proceedings of the IEEE/CVF Winter Conference on Applications of Computer Vision*, pages 5551–5563, 2023.
- Mayu Sakurada and Takehisa Yairi. Anomaly detection using autoencoders with nonlinear dimensionality reduction. In *Proceedings of the MLSDA 2014 2nd workshop on machine learning for sensory data analysis*, pages 4–11, 2014.
- Bo Zong, Qi Song, Martin Renqiang Min, Wei Cheng, Cristian Lumezanu, Daeki Cho, and Haifeng Chen. Deep autoencoding gaussian mixture model for unsupervised anomaly detection. In *International conference on learning representations*, 2018.
- Chong Zhou and Randy C Paffenroth. Anomaly detection with robust deep autoencoders. In *Proceedings of the 23rd ACM SIGKDD international conference on knowledge discovery and data mining*, pages 665–674, 2017.
- Thomas Schlegl, Philipp Seeböck, Sebastian M Waldstein, Ursula Schmidt-Erfurth, and Georg Langs. Unsupervised anomaly detection with generative adversarial networks to guide marker discovery. In *International conference on information processing in medical imaging*, pages 146–157. Springer, 2017.
- Houssam Zenati, Chuan Sheng Foo, Bruno Lecouat, Gaurav Manek, and Vijay Ramaseshan Chandrasekhar. Efficient gan-based anomaly detection. *arXiv preprint arXiv:1802.06222*, 2018.
- Djennifer K Madzia-Madzou and Hugo J Kuijf. Progressive ganomaly: anomaly detection with progressively growing gans. In *Medical Imaging 2022: Image Processing*, volume 12032, pages 527–540. SPIE, 2022.
- Mingxing Tan and Quoc Le. Efficientnet: Rethinking model scaling for convolutional neural networks. In *International conference on machine learning*, pages 6105–6114. PMLR, 2019.
- Luai Al Shalabi, Zyad Shaaban, and Basel Kasasbeh. Data mining: A preprocessing engine. *Journal of Computer Science*, 2(9):735–739, 2006.
- Yibo Zhou. Rethinking reconstruction autoencoder-based out-of-distribution detection. In *Proceedings of the IEEE/CVF Conference on Computer Vision and Pattern Recognition*, pages 7379–7387, 2022.
- Yuxin Wu and Kaiming He. Group normalization. In *Proceedings of the European conference on computer vision (ECCV)*, pages 3–19, 2018.

- Jiaming Song, Chenlin Meng, and Stefano Ermon. Denoising diffusion implicit models. *arXiv* preprint arXiv:2010.02502, 2020.
- Alex Krizhevsky, Geoffrey Hinton, et al. Learning multiple layers of features from tiny images. 2009.
- Ziwei Liu, Ping Luo, Xiaogang Wang, and Xiaoou Tang. Deep learning face attributes in the wild. In *Proceedings of the IEEE international conference on computer vision*, pages 3730–3738, 2015.
- Yuval Netzer, Tao Wang, Adam Coates, Alessandro Bissacco, Baolin Wu, Andrew Y Ng, et al. Reading digits in natural images with unsupervised feature learning. In *NIPS workshop on deep learning and unsupervised feature learning*, volume 2011, page 7. Granada, Spain, 2011.
- Jianxiong Xiao, James Hays, Krista A Ehinger, Aude Oliva, and Antonio Torralba. Sun database: Large-scale scene recognition from abbey to zoo. In 2010 IEEE computer society conference on computer vision and pattern recognition, pages 3485–3492. IEEE, 2010.
- Fisher Yu, Ari Seff, Yinda Zhang, Shuran Song, Thomas Funkhouser, and Jianxiong Xiao. Lsun: Construction of a large-scale image dataset using deep learning with humans in the loop. *arXiv* preprint arXiv:1506.03365, 2015.
- Pingmei Xu, Krista A Ehinger, Yinda Zhang, Adam Finkelstein, Sanjeev R Kulkarni, and Jianxiong Xiao. Turkergaze: Crowdsourcing saliency with webcam based eye tracking. arXiv preprint arXiv:1504.06755, 2015.
- Grant Van Horn, Oisin Mac Aodha, Yang Song, Yin Cui, Chen Sun, Alex Shepard, Hartwig Adam, Pietro Perona, and Serge Belongie. The inaturalist species classification and detection dataset. In *Proceedings of the IEEE conference on computer vision and pattern recognition*, pages 8769–8778, 2018.
- Mircea Cimpoi, Subhransu Maji, Iasonas Kokkinos, Sammy Mohamed, and Andrea Vedaldi. Describing textures in the wild. In *Proceedings of the IEEE conference on computer vision and pattern recognition*, pages 3606–3613, 2014.
- Bolei Zhou, Agata Lapedriza, Aditya Khosla, Aude Oliva, and Antonio Torralba. Places: A 10 million image database for scene recognition. *IEEE transactions on pattern analysis and machine intelligence*, 40(6):1452–1464, 2017.
- Li Deng. The mnist database of handwritten digit images for machine learning research [best of the web]. *IEEE signal processing magazine*, 29(6):141–142, 2012.
- Tarin Clanuwat, Mikel Bober-Irizar, Asanobu Kitamoto, Alex Lamb, Kazuaki Yamamoto, and David Ha. Deep learning for classical japanese literature. *arXiv preprint arXiv:1812.01718*, 2018.
- Brenden M Lake, Ruslan Salakhutdinov, and Joshua B Tenenbaum. Human-level concept learning through probabilistic program induction. *Science*, 350(6266):1332–1338, 2015.
- Kaiming He, Xiangyu Zhang, Shaoqing Ren, and Jian Sun. Deep residual learning for image recognition. In *Proceedings of the IEEE conference on computer vision and pattern recognition*, pages 770–778, 2016.
- Jia Deng, Wei Dong, Richard Socher, Li-Jia Li, Kai Li, and Li Fei-Fei. Imagenet: A large-scale hierarchical image database. In 2009 IEEE conference on computer vision and pattern recognition, pages 248–255. Ieee, 2009.
- Zhisheng Xiao, Qing Yan, and Yali Amit. Do we really need to learn representations from in-domain data for outlier detection? *arXiv preprint arXiv:2105.09270*, 2021.

Appendix

Supplementary Algorithm

This section provides two key algorithms used for evaluating our approach: the MSE (Mean Squared Error) calculation and the Likelihood Regret (LR) calculation.

The MSE calculation, as shown in Algorithm 3, computes the mean squared error between the original and reconstructed latent features. It serves as a basic measure of reconstruction error for detecting OOD samples.

The LR calculation, detailed in Algorithm 4, measures the reduction in reconstruction error by comparing the MSE values at the initial and final epochs of training. This metric reflects how well the model has adapted to the ID data over time, with a higher reduction indicating better adaptation.

Algorithm 3 Testing Algorithm for MSE Calculation

```
1: Input: An image x
```

2: Output: MSE score

3: $\mathbf{z}_0 = \mathcal{H}(\mathbf{x})$

4: $\mathbf{z}_t \leftarrow \text{ennoise}(\mathbf{z}_0)$

5: $\tilde{\mathbf{z}}_0 = \text{denoise}(\mathbf{z}_t, t)$

6: MSE $\leftarrow \frac{1}{N}\sum_{i=1}^{N}(\mathbf{z}_0[i] - \tilde{\mathbf{z}}_0[i])^2$ 7: **return** MSE

 $\triangleright i$ indexes the elements of \mathbf{z}_0 and $\tilde{\mathbf{z}}_0$

Algorithm 4 Testing Algorithm for LR Calculation

```
1: Input: An image x, MSE at initial and final epochs
```

2: Output: LR score

2: **Output:** LR score

3: $\mathbf{z}_0^{\text{initial}} = \mathcal{H}(\mathbf{x})$ at the beginning of training

4: $\mathbf{z}_t^{\text{initial}} \leftarrow \text{ennoise}(\mathbf{z}_0^{\text{initial}})$ 5: $\tilde{\mathbf{z}}_0^{\text{initial}} = \text{denoise}(\mathbf{z}_t^{\text{initial}}, t)$ 6: $\text{MSE}_{\text{initial}} \leftarrow \frac{1}{N} \sum_{i=1}^{N} (\mathbf{z}_0^{\text{initial}}[i] - \tilde{\mathbf{z}}_0^{\text{initial}}[i])^2$ 7: $\mathbf{z}_0^{\text{final}} = \mathcal{H}(\mathbf{x})$ at the end of training

8: $\mathbf{z}_t^{\text{final}} \leftarrow \text{ennoise}(\mathbf{z}_0^{\text{final}})$ 9: $\tilde{\mathbf{z}}_0^{\text{inal}} = \text{denoise}(\mathbf{z}_t^{\text{final}}, t)$ 10: $\text{MSE}_{\text{final}} \leftarrow \frac{1}{N} \sum_{i=1}^{N} (\mathbf{z}_0^{\text{final}}[i] - \tilde{\mathbf{z}}_0^{\text{final}}[i])^2$ 11: $\text{LR} \leftarrow \text{MSE}_{\text{initial}} - \text{MSE}_{\text{final}}$

12: return LR

В **More Experimental Details**

Dataset Details and Testing Speeds

Table 1: CIFAR-10 Dataset The CIFAR-10 test set consisted of 10,000 images. The SVHN dataset contained 26,032 images, LSUN-r had 10,000 images, and Fashion-MNIST, MNIST, and KMNIST each comprised 10,000 images. Omniglot included 13,180 images, and notMNIST had 18,724 images, totaling 97,936 OOD samples. The testing of the MFsim metric took a total of 98 seconds, with an average speed of 999.3 images per second.

Table 2 : CelebA Dataset The CelebA test set comprised 60,780 images, SUN included 10,000 images, iNaturalist had 100,000 images, Textures consisted of 1,678 images, and Places365 had 1,002 images, making up a total of 112,680 OOD samples. Testing the MFsim metric took a total of 109 seconds, processing an average of 1033.8 images per second.

B.2 Training Details

Both CIFAR-10 and CelebA datasets were trained for 200 epochs using the VAE model. The GLOW model was trained for 150 epochs with a learning rate of 5×10^{-4} , and PixelCNN+ was trained for 150 epochs at the same learning rate. Under the DDPM model, both datasets were trained for 350 epochs, following the experimental setups and code provided in the original papers. We used LFDN without time-step embeddings as our autoencoder, used MFsim metrics, and kept all remaining training details consistent with our approach.

C Supplementary Experiments

C.1 Experimental Results for FPR95 Values Using EfficientNet-b4 as Backbone

We conducted tests to evaluate the FPR95 (False Positive Rate at 95% True Positive Rate) values using CIFAR10 and CIFAR100 datasets as in-distribution data while treating the remaining six datasets as out-of-distribution datasets. The specific FPR95 values are summarized in **Table 5**.

Table 5: The FPR95 values for OOD detection, where CIFAR-10/100 is used as the in-distribution dataset. The results are compared with Classification-based and Distance-based methods using EfficientNet-b4 as the backbone. Higher AUROC values indicate better performance, with the best results highlighted in bold for clarity.

	l	l	l			00	D			
ID	Based	Method	Num img/s (†)	SVHN	LSUN-c	LSUN-r	iSUN	Textures	Places365	average
	I	MSP	1060.5	43.99	26.13	48.65	46.89	27.50	15.03	34.70
		EBO	1060.5	16.51	11.52	28.38	27.03	16.08	4.99	17.42
	Classifier-based	DICE	1066.3	7.70	4.81	25.74	21.76	7.80	1.49	11.55
		ASH-S	1047.6	6.89	4.15	31.29	26.29	5.21	1.32	12.53
CIFAR10		SimCLR+Mahalanobis	674.8	9.24	67.73	75.43	64.32	56.22	72.15	57.52
CHARIO	Distance-based	SimCLR+KNN	919.8	49.15	54.89	76.97	73.48	15.27	39.39	51.53
i	Generative-based	ours(+MSE)	960.6	21.15±0.03	19.52±0.01	39.67±0.02	43.76±0.02	0±0.00	0.42±0.03	20.75±0.02
		ours(+LR)	360.2	14.26±0.02	18.67 ± 0.03	31.62 ± 0.02	37.76 ± 0.02	0.06 ± 0.01	0.83 ± 0.02	17.20±0.02
		ours(+MFsim)	960.6	4.34±0.02	0.04 ± 0.01	4.42 ± 0.02	6.26 ± 0.02	0 ± 0.00	0 ± 0.00	2.51 ± 0.01
		MSP	1060.5	80.10	68.80	80.35	80.36	47.11	57.41	69.02
		EBO	1060.5	88.74	78.64	72.35	76.57	95.83	94.04	84.36
	Classifier-based	DICE	1066.3	63.77	58.96	77.89	78.67	34.26	48.77	60.39
		ASH-S	1047.6	34.28	44.39	89.45	86.13	21.44	34.59	51.71
CIFAR 100	L	SimCLR+Mahalanobis	674.8	94.95	96.35	85.05	86.29	80.37	95.50	89.75
CHIMCIOO	Distance-based	SimCLR+KNN	919.8	95.32	97.11	78.45	84.38	95.28	94.82	90.89
		ours(+MSE)	960.6	89.05±0.02	69.14 ± 0.03	69.63 ± 0.02	89.79 ± 0.01	$0.12{\pm}0.02$	0 ± 0.00	52.95±0.02
	Generative-based	ours(+LR)	360.2	62.06±0.03	72.19 ± 0.04	86.67 ± 0.02	86.17 ± 0.02	0.42 ± 0.02	2.81 ± 0.02	51.72±0.03
CIFAR100		ours(+MFsim)	960.6	37.48±0.02	1.90 ± 0.01	23.05 ± 0.02	26.00 ± 0.02	0 ± 0.00	0 ± 0.00	14.78±0.02

As shown in **Table 5**, our method demonstrates a significant advantage in terms of FPR95 values compared to other classification-based and distance-based approaches. Specifically, when using CIFAR100 as in-distribution data, our method achieves an average reduction of 36.93% in FPR95 values compared to the state-of-the-art classification-based approach, ASH-S.

C.2 Experimental Results with ResNet50 as Encoder

Besides using EfficientNet-b4 as the encoder, we also employed the commonly used ResNet50 to extract multi-layer semantic features. For ResNet50, feature maps from stages 1 to 3 were selected, with channel counts of 256, 512, and 1024, respectively. These feature maps were concatenated to form a 1792-dimensional vector, which was then used as input for the LFDN. The results for three OOD detection metrics are presented in **Table 6** and **Table 7**. Both tables compare our method with classification-based and distance-based methods.

As shown in **Table 6** and **Table 7**, when using ResNet50 as the backbone, our method still achieves the best performance. Specifically, with CIFAR-10 as the in-distribution dataset, the average AUROC and MFsim values are 98.30% and 8.89%, respectively, outperforming the classification-based SOTA method DICE by 6.17% in AUROC and reducing the FPR95 by 24.43%.

Figures 6 and 7 illustrate the differences in the MFsim score distributions for various datasets, with ResNet50 as the encoder and CIFAR10 as the in-distribution dataset, across the first and last epochs.

Table 6: The AUROC values for OOD detection, where CIFAR-10/100 is used as the in-distribution dataset. The results are compared with Classification-based and Distance-based methods using ResNet50 as the backbone. Higher AUROC values indicate better performance, with the best results highlighted in bold for clarity.

,						OOI)			
ID	Based	Method	Num img/s (†)	SVHN	LSUN-c	LSUN-r	iSUN	Textures	Places365	average
		MSP	1321.5	80.64	95.05	91.65	89.95	87.78	90.43	89.25
		EBO	1321.5	81.90	98.21	94.43	93.09	86.84	92.45	91.15
	Classifier-based	DICE	1369.3	91.92	99.18	91.13	90.51	87.39	92.66	92.13
		ASH-S	1307.4	84.16	98.76	95.00	94.40	87.88	91.63	91.97
CIFAR10		SimCLR+Mahalanobis	857.2	90.17	73.74	86.14	83.25	81.48	91.23	84.34
CIFARIO	Distance-based	SimCLR+KNN	1179.8	92.36	91.13	87.78	91.82	88.62	79.41	88.52
	Generative-based	ours(+MSE)	654.9	81.40	94.02	81.11	81.36	100.00	100.00	89.65
		ours(+LR)	296.7	90.95	92.53	85.22	85.91	100.00	100.00	92.44
	Generalive based	ours(+MFsim)	654.9	95.98±0.02	99.86 \pm 0.02	97.06 ± 0.02	96.89 ± 0.01	100 ± 0.00	100 ± 0.00	98.30±0.01
		MSP	1321.5	78.38	84.18	78.98	78.09	76.54	72.00	78.03
		EBO	1321.5	83.13	89.35	83.83	83.35	78.85	71.42	81.66
	Classifier-based	DICE	1369.3	87.93	93.32	82.41	82.20	79.29	69.65	82.47
		ASH-S	1307.4	91.66	93.24	69.93	72.78	87.75	71.00	81.06
CIFAR100		SimCLR+Mahalanobis	857.2	91.92	57.14	87.47	88.00	94.96	71.86	81.89
CITTICTOO	Distance-based	SimCLR+KNN	1179.8	87.78	84.30	82.51	77.69	83.35	73.74	81.56
		ours(+MSE)	654.9	86.55	99.11	93.02	91.87	100.00	100.00	95.09
	Generative-based	ours(+LR)	296.7	89.17	99.16	93.65	92.33	100.00	100.00	95.72
		ours(+MFsim)	654.9	89.68±0.02	99.18 \pm 0.01	93.64 ± 0.02	92.94 ± 0.02	100 ± 0.00	100 ± 0.00	95.91±0.01

Table 7: The FPR95 values for OOD detection, where CIFAR-10/100 is used as the in-distribution dataset. The results are compared with Classification-based and Distance-based methods using ResNet50 as the backbone. Higher AUROC values indicate better performance, with the best results highlighted in bold for clarity.

						OC	D			
ID	Based	Method	Num img/s (†)	SVHN	LSUN-c	LSUN-r	iSUN	Textures	Places365	average
		MSP	1321.5	60.56	16.09	28.21	35.63	45.4	32.93	36.47
		EBO	1321.5	59.15	8.07	23.79	30.72	60.2	31.66	35.60
	Classifier-based	DICE	1369.3	27.07	4.11	37.83	41.12	57.48	32.32	33.32
		ASH-S	1307.4	53.93	5.57	20.29	22.31	64.36	39.71	34.36
CIFAR10		SimCLR+Mahalanobis	857.2	27.65	33.35	48.17	51.22	38.12	60.43	43.16
	Distance-based	SimCLR+KNN	1179.8	24.53	25.29	37.81	27.55	34.36	62.19	35.29
	Generative-based	ours(+MSE)	654.9	94.79	45.99	95.86	91.68	0.00	0.00	54.72
		ours(+LR)	296.7	34.59	25.77					28.16
		ours(+MFsim)	654.9	21.10 ± 0.03	0.02 ± 0.01	15.75 ± 0.03	LSUN-r iSUN Textures Places365 a	8.89±0.02		
		MSP	1321.5	53.38	43.52	56.23	57.69	63.63	77.53	58.66
	CI :C 1 1	EBO	1321.5	47.04	34.15	51.14	52.36	63.05	80.95	54.78
	Classifier-based	DICE	1369.3	38.7	28.77	56.21	56.74	65.21	82.63	54.71
		ASH-S	1307.4	29.83	28.75	89.48	85.22	51.8	81.48	61.09
CIFAR100		SimCLR+Mahalanobis	857.2	32.19	80.43	39.93	40.39	28.21	81.44	50.43
	Distance-based	SimCLR+KNN	1179.8	39.23	48.99	60.21	74.99	57.15	80.74	60.22
		ours(+MSE)	654.9	78.54	0.49					27.33
	Generative-based	ours(+LR)	296.7	65.93	0.57	36.71	38.78	0.00	0.00	23.67
		ours(+MFsim)	654.9	64.72±0.03	1.08 ± 0.02	39.66 ± 0.04	39.79 ± 0.03	0.00 ± 0.00	0.00 ± 0.00	24.21±0.02

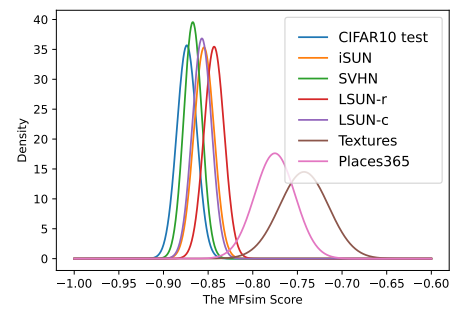


Figure 6: The MFsim score distributions of the First Epoch with ResNet50 as Encoder

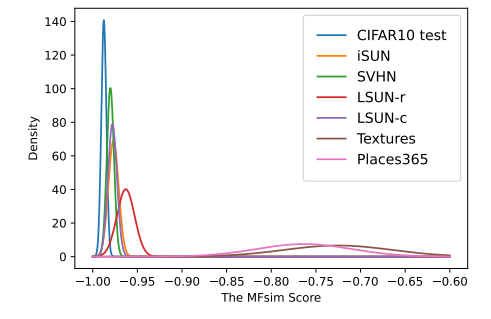


Figure 7: The MFsim score distributions of the Last Epoch with ResNet50 as Encoder

C.3 CIFAR-10 as ID and CIFAR-100 as OOD

As shown in **Table 8**, when CIFAR-10 is used as the ID dataset and CIFAR-100 as the OOD dataset, our method consistently achieves the best performance across different evaluation metrics, including AUROC and FPR95. Compared to classification-based methods, the improvement is not significantly large, but our approach still shows a consistent edge, particularly in feature-generative-based models, demonstrating the robustness of our method.

Table 8: The FPR95 and AUROC Values for CIFAR-10 as ID Samples and CIFAR100 as OOD Samples.

ID	OOD	Based	Method	FPR95↓	AUROC↑
	CIFAR100	Classification-Based	MSP EBO ASH-S	52.04 51.32 51.29	86.14 86.19 87.13
CIFAR10		Pixel-Generative-Based	GLOW VAE DDPM	90.41 67.38	73.60 55.95 82.43
		Feature-Generative-Based	ours(+MSE) ours(+LR) ours(+MFsim)	48.87 49.48 53.70	87.54 87.24 85.60

C.4 Comparisons with recent generative methods

The comparison between our method and DDPM[Graham et al., 2023] can be referred to **Table 1** and **Table 2**. Our method outperforms DDPM consistently on benchmarks using CIFAR10 or CelebA as ID data.

The comparison between our method and Diffuard[Gao et al., 2023] is provided in **Table 9**. Results of Diffuard are taken from its original paper. Here, CIFAR10 is regarded as ID data, while CIFAR100 or TinyImagenet is regarded as OOD data. Our method based on MFsim achieves overall better performance than 'Diffuard+Deep Ens', with 1.55 higher AUROC and 21.77 lower FPR95.

The comparison between our method and LMD[Liu et al., 2023] is shown in **Table 10**. The evaluation metric is AUROC. The average AUROC of our method based on MFsim is 6.94 higher than that of LMD.

Table 9: The AUROC and FPR95 values compared to DiffGuard [Gao et al., 2023] using CIFAR-10 as the ID dataset and CIFAR-100/TinyImageNet as the OOD datasets.

	CIFAR-100		TINYIMA	GENET	aver	age
Method	AUROC↑	FPR95↓	AUROC↑	FPR95↓	AUROC↑	FPR95↓
Diffuard	89.88	52.67	91.88	45.48	90.88	49.08
Diffuard+EBO	89.93	50.77	91.95	43.58	90.94	47.18
Diffuaed+Deep Ens	90.40	52.51	91.98	45.04	91.19	48.78
ours(+MSE)	87.54	48.87	97.68	13.42	92.61	31.15
ours(+LR)	87.24	49.48	97.11	15.04	92.18	32.26
ours(+MFsim)	85.60	53.70	99.88	0.39	92.74	27.01

C.5 Comparison against other methods using the multi-scale feature encodings as the input.

In **Table 11**, we have made comparison of our method against AE and VAE using the multi-layer feature encodings as inputs. For AE (AutoEncoder), we use the LFDN network without the timestep embedding, i.e., a 16-layer linear network. For VAE, we use a 5-layer linear network as the encoder

Table 10: The AUROC values compared to LMD [Liu et al., 2023] using CIFAR-10/CIFAR-100 as the ID dataset and CIFAR-100/CIFAR10/SVHN as the OOD datasets.

ID	OOD	LMD	ours(+MSE)	ours(+LR)	ours(+MFsim)
CIEA D 10	CIFAR100	60.70	87.54	87.24	85.6
CIFAR10	SVHN	99.20	97.31	98.22	98.89
	CIFAR10	56.80	70.52	72.86	64.58
CIFAR100	SVHN	98.50	83.93	88.84	93.9
AVERAGE		78.80	84.83	86.79	85.74

and an 8-layer linear network as the decoder. Compared to AE and VAE, the diffusion model has significant advantages when modeling complex multidimensional distributions.

C.6 Comparisons with pixel-level denoising approaches.

We provide the distribution differences of the MSE score and MFsim score at two levels after training, with CIFAR-10 as ID dataset and other datasets as OOD; The results are shown in Figures 8 and 9.

It can be observed that at the pixel level(DDPM), the reconstruction error distributions of ID and OOD samples are very similar. The mixed MSE scores make it very hard to distinguish ID samples from OOD samples. However, at the feature level, the reconstruction score distribution of ID samples shows a clear distinction from that of OOD samples. The reason is that, our feature-level diffusion-based generative model makes the projected in-distribution latent space not only be compressed sufficiently to capture the exclusive characteristics of ID images, but also provide sufficient reconstruction power for the large-scale ID images of various categories. In other words, the pretrained encoder has inherent generalization capabilities, and the multi-layer features it extracts are more discriminative than the high-dimensional pixels of the images themselves.

Table 11: The AUROC values compared to the other generative models using CIFAR-10 as the ID dataset.

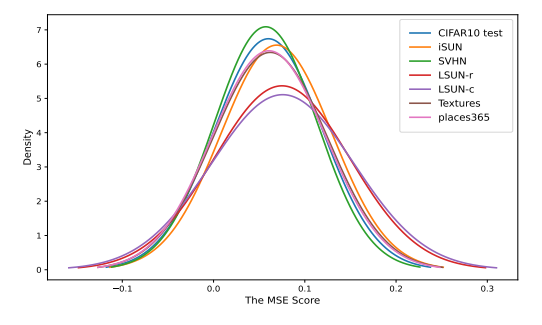
	Dataset		Method	
ID	OOD	AE(+MFsim)	VAE(+MFsim)	Diffusion(+MFsim)
CIFRA10	SVHN LSUN MNIST FMNIST KMNIST Omniglot NotMNIST	57.68 81.47 95.85 79.61 90.51 81.50 81.61	83.96 97.69 99.98 98.69 99.96 97.69 99.88	98.89 99.83 99.99 99.99 99.99 99.99
	average	81.18	96.84	99.81
Time	Num img/s (↑)	1224.2	1179.4	999.3

C.7 ImageNet100 as ID Dataset

In **Table 12**, our method using MSE outperforms the classification-based SOTA method DICE, achieving an improvement of 3.91% in AUROC when ImageNet100 is used as the ID dataset and various datasets such as SUN, iNaturalist, Textures, and Places365 are used as OOD datasets. The significant improvements in performance metrics demonstrate that our generative-based approach can effectively model the in-distribution characteristics, leading to better OOD detection capabilities. This indicates that our proposed method is particularly suitable for more complex datasets like ImageNet100, where capturing detailed features is crucial for accurate OOD detection.

Table 12: The AUROC and FPR95 Values for Different Methods with ImageNet100 as ID Dataset and SUN/iNaturalist/Textures/Places365 as OOD Datasets.

ID	Method	# img/s (†)	SU	N	iNatu	iNaturalist		Textures		Places365		Average	
			AUROC↑	FPR95↓	AUROC↑	FPR95↓	AUROC↑	FPR95↓	AUROC↑	FPR95↓	AUROC↑	FPR95↓	
	MSP	956.2	89.68	52.16	86.44	57.88	86.48	55.18	88.85	53.79	87.86	54.75	
	EBO	956.2	90.83	49.46	87.82	58.29	86.04	66.81	90.01	51.80	88.68	56.59	
	DICE	950.8	93.78	37.14	89.76	50.47	89.52	52.32	93.18	41.42	91.56	45.34	
ImageNet100	ASH-S	977.5	90.12	44.54	86.94	51.45	88.38	45.23	88.76	49.70	88.55	47.73	
imageretroo	ours(+MSE)	954.9	98.81	5.91	86.59	71.88	97.68	10.76	98.79	5.73	95.47	23.57	
	ours(+LR)	313.4	93.98	16.51	51.39	87.99	76.02	47.54	94.95	16.25	79.09	42.07	
	ours(+MFsim)	954.9	98.49	8.41	84.63	77.86	98.08	9.98	98.37	8.75	94.89	26.25	



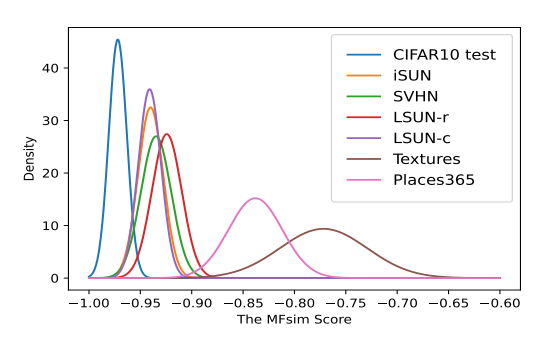


Figure 8: Reconstruction Error Distribution of ID and OOD Samples for Pixel-level

Figure 9: Reconstruction Error Distribution of ID and OOD Samples for Feature-level

D Qualitative results.

We have included three types of failure cases Figures 10, 11 and 12. The first type, shown in Figure 10, represents ID samples misclassified as OOD. It can be observed that these misclassified samples often have significant shadows and lack semantic information, resulting in high reconstruction errors and being incorrectly classified as OOD samples. The second type, shown in Figure 11, represents OOD samples misclassified as ID. It can be observed that these OOD samples have categories very similar to those of the ID samples (CIFAR-10), such as cars and ships, which are categories present in CIFAR-10. The third type, shown in Figure 12, represents OOD samples with colors very similar to the ID samples, leading to their misclassification as ID.



Figure 10: Examples of ID Samples Misclassified as OOD (Lacking Semantic Information).



Figure 11: Examples of OOD Samples Misclassified as ID (Similar to ID Sample Categories).



Figure 12: Examples of OOD Samples Misclassified as ID (Similar to ID Sample Colors).

NeurIPS Paper Checklist

1. Claims

Question: Do the main claims made in the abstract and introduction accurately reflect the paper's contributions and scope?

Answer: [Yes] Yes

Justification: The main claims in the abstract and introduction accurately reflect our contributions. We propose a diffusion-based layer-wise semantic reconstruction method for unsupervised out-of-distribution (OOD) detection. Our method demonstrates superior performance in detecting OOD samples, as detailed in Section 3 and Section 4of our paper.

Guidelines:

- The answer NA means that the abstract and introduction do not include the claims made in the paper.
- The abstract and/or introduction should clearly state the claims made, including the
 contributions made in the paper and important assumptions and limitations. A No or
 NA answer to this question will not be perceived well by the reviewers.
- The claims made should match theoretical and experimental results, and reflect how much the results can be expected to generalize to other settings.
- It is fine to include aspirational goals as motivation as long as it is clear that these goals are not attained by the paper.

2. Limitations

Question: Does the paper discuss the limitations of the work performed by the authors?

Answer: [Yes] Yes

Justification: The limitations of our work are discussed in detail in Section 5

- The answer NA means that the paper has no limitation while the answer No means that the paper has limitations, but those are not discussed in the paper.
- The authors are encouraged to create a separate "Limitations" section in their paper. , but those are not discussed in the paper.
- The authors are encouraged to create a separate "Limitations" section in their paper.
- The paper should point out any strong assumptions and how robust the results are to violations of these assumptions (e.g., independence assumptions, noiseless settings, model well-specification, asymptotic approximations only holding locally). The authors should reflect on how these assumptions might be violated in practice and what the implications would be.
- The authors should reflect on the scope of the claims made, e.g., if the approach was only tested on a few datasets or with a few runs. In general, empirical results often depend on implicit assumptions, which should be articulated.
- The authors should reflect on the factors that influence the performance of the approach. For example, a facial recognition algorithm may perform poorly when image resolution is low or images are taken in low lighting. Or a speech-to-text system might not be used reliably to provide closed captions for online lectures because it fails to handle technical jargon.
- The authors should discuss the computational efficiency of the proposed algorithms and how they scale with dataset size.
- If applicable, the authors should discuss possible limitations of their approach to address problems of privacy and fairness.
- While the authors might fear that complete honesty about limitations might be used by reviewers as grounds for rejection, a worse outcome might be that reviewers discover limitations that aren't acknowledged in the paper. The authors should use their best judgment and recognize that individual actions in favor of transparency play an important role in developing norms that preserve the integrity of the community. Reviewers will be specifically instructed to not penalize honesty concerning limitations.

3. Theory Assumptions and Proofs

Question: For each theoretical result, does the paper provide the full set of assumptions and a complete (and correct) proof?

Answer: [NA] N/A

Justification: Our paper focuses on an experimental approach to out-of-distribution detection and does not include theoretical results. Therefore, this question is not applicable.

Guidelines:

- The answer NA means that the paper does not include theoretical results.
- All the theorems, formulas, and proofs in the paper should be numbered and crossreferenced.
- All assumptions should be clearly stated or referenced in the statement of any theorems.
- The proofs can either appear in the main paper or the supplemental material, but if they appear in the supplemental material, the authors are encouraged to provide a short proof sketch to provide intuition.
- Inversely, any informal proof provided in the core of the paper should be complemented by formal proofs provided in appendix or supplemental material.
- Theorems and Lemmas that the proof relies upon should be properly referenced.

4. Experimental Result Reproducibility

Question: Does the paper fully disclose all the information needed to reproduce the main experimental results of the paper to the extent that it affects the main claims and/or conclusions of the paper (regardless of whether the code and data are provided or not)?

Answer: [Yes] Yes

Justification: Our paper fully discloses all necessary information to reproduce the main experimental results, including detailed descriptions of the experimental setup, datasets used, and evaluation metrics. This information is provided in Sections 4 of the paper.

- The answer NA means that the paper does not include experiments.
- If the paper includes experiments, a No answer to this question will not be perceived well by the reviewers: Making the paper reproducible is important, regardless of whether the code and data are provided or not.
- If the contribution is a dataset and/or model, the authors should describe the steps taken to make their results reproducible or verifiable.
- Depending on the contribution, reproducibility can be accomplished in various ways. For example, if the contribution is a novel architecture, describing the architecture fully might suffice, or if the contribution is a specific model and empirical evaluation, it may be necessary to either make it possible for others to replicate the model with the same dataset, or provide access to the model. In general, releasing code and data is often one good way to accomplish this, but reproducibility can also be provided via detailed instructions for how to replicate the results, access to a hosted model (e.g., in the case of a large language model), releasing of a model checkpoint, or other means that are appropriate to the research performed.
- While NeurIPS does not require releasing code, the conference does require all submissions to provide some reasonable avenue for reproducibility, which may depend on the nature of the contribution. For example
 - (a) If the contribution is primarily a new algorithm, the paper should make it clear how to reproduce that algorithm.
 - (b) If the contribution is primarily a new model architecture, the paper should describe the architecture clearly and fully.
 - (c) If the contribution is a new model (e.g., a large language model), then there should either be a way to access this model for reproducing the results or a way to reproduce the model (e.g., with an open-source dataset or instructions for how to construct the dataset).

(d) We recognize that reproducibility may be tricky in some cases, in which case authors are welcome to describe the particular way they provide for reproducibility. In the case of closed-source models, it may be that access to the model is limited in some way (e.g., to registered users), but it should be possible for other researchers to have some path to reproducing or verifying the results.

5. Open access to data and code

Question: Does the paper provide open access to the data and code, with sufficient instructions to faithfully reproduce the main experimental results, as described in supplemental material?

Answer: [Yes] Yes

Justification: We have provided open access to our data and code, along with detailed instructions for reproducing the main experimental results. These resources are described in the supplemental material and can be accessed via the provided links.

Guidelines:

- The answer NA means that paper does not include experiments requiring code.
- Please see the NeurIPS code and data submission guidelines (https://nips.cc/public/guides/CodeSubmissionPolicy) for more details.
- While we encourage the release of code and data, we understand that this might not be possible, so "No" is an acceptable answer. Papers cannot be rejected simply for not including code, unless this is central to the contribution (e.g., for a new open-source benchmark).
- The instructions should contain the exact command and environment needed to run to reproduce the results. See the NeurIPS code and data submission guidelines (https://nips.cc/public/guides/CodeSubmissionPolicy) for more details.
- The authors should provide instructions on data access and preparation, including how
 to access the raw data, preprocessed data, intermediate data, and generated data, etc.
- The authors should provide scripts to reproduce all experimental results for the new proposed method and baselines. If only a subset of experiments are reproducible, they should state which ones are omitted from the script and why.
- At submission time, to preserve anonymity, the authors should release anonymized versions (if applicable).
- Providing as much information as possible in supplemental material (appended to the paper) is recommended, but including URLs to data and code is permitted.

6. Experimental Setting/Details

Question: Does the paper specify all the training and test details (e.g., data splits, hyperparameters, how they were chosen, type of optimizer, etc.) necessary to understand the results?

Answer: [Yes] Yes

Justification: Our paper specifies all necessary training and test details, including data splits, hyperparameters, and optimizer settings. These details are provided in Section 4.

Guidelines:

- The answer NA means that the paper does not include experiments.
- The experimental setting should be presented in the core of the paper to a level of detail that is necessary to appreciate the results and make sense of them.
- The full details can be provided either with the code, in appendix, or as supplemental
 material.

7. Experiment Statistical Significance

Question: Does the paper report error bars suitably and correctly defined or other appropriate information about the statistical significance of the experiments?

Answer: [Yes] Yes

Justification: We have reported error bars for our main experimental results, calculated as the mean and standard deviation over three runs. Details on the calculation of error bars and the factors of variability considered (such as train/test split and random initialization) are provided in Section 4.

Guidelines:

- The answer NA means that the paper does not include experiments.
- The authors should answer "Yes" if the results are accompanied by error bars, confidence intervals, or statistical significance tests, at least for the experiments that support the main claims of the paper.
- The factors of variability that the error bars are capturing should be clearly stated (for example, train/test split, initialization, random drawing of some parameter, or overall run with given experimental conditions).
- The method for calculating the error bars should be explained (closed form formula, call to a library function, bootstrap, etc.)
- The assumptions made should be given (e.g., Normally distributed errors).
- It should be clear whether the error bar is the standard deviation or the standard error of the mean.
- It is OK to report 1-sigma error bars, but one should state it. The authors should preferably report a 2-sigma error bar than state that they have a 96% CI, if the hypothesis of Normality of errors is not verified.
- For asymmetric distributions, the authors should be careful not to show in tables or figures symmetric error bars that would yield results that are out of range (e.g. negative error rates).
- If error bars are reported in tables or plots, The authors should explain in the text how they were calculated and reference the corresponding figures or tables in the text.

8. Experiments Compute Resources

Question: For each experiment, does the paper provide sufficient information on the computer resources (type of compute workers, memory, time of execution) needed to reproduce the experiments?

Answer: [Yes] Yes

Justification: The paper provides detailed information on the compute resources used for the experiments, including the type of compute workers (GPU), memory, and execution time. These details are specified in the experimental setup section 4.

Guidelines:

- The answer NA means that the paper does not include experiments.
- The paper should indicate the type of compute workers CPU or GPU, internal cluster, or cloud provider, including relevant memory and storage.
- The paper should provide the amount of compute required for each of the individual experimental runs as well as estimate the total compute.
- The paper should disclose whether the full research project required more compute than the experiments reported in the paper (e.g., preliminary or failed experiments that didn't make it into the paper).

9. Code Of Ethics

Question: Does the research conducted in the paper conform, in every respect, with the NeurIPS Code of Ethics https://neurips.cc/public/EthicsGuidelines?

Answer: [Yes] Yes

Justification: We have thoroughly reviewed the NeurIPS Code of Ethics and confirm that our research conforms to these guidelines in every respect.

- The answer NA means that the authors have not reviewed the NeurIPS Code of Ethics.
- If the authors answer No, they should explain the special circumstances that require a deviation from the Code of Ethics.

The authors should make sure to preserve anonymity (e.g., if there is a special consideration due to laws or regulations in their jurisdiction).

10. Broader Impacts

Question: Does the paper discuss both potential positive societal impacts and negative societal impacts of the work performed?

Answer: [Yes] Yes

Justification: We discuss the potential positive and negative societal impacts of our work in Section 7. Specifically, we address how our method could improve unsupervised out-of-distribution detection, as well as the potential risks associated with misuse in surveillance applications.

Guidelines:

- The answer NA means that there is no societal impact of the work performed.
- If the authors answer NA or No, they should explain why their work has no societal impact or why the paper does not address societal impact.
- Examples of negative societal impacts include potential malicious or unintended uses (e.g., disinformation, generating fake profiles, surveillance), fairness considerations (e.g., deployment of technologies that could make decisions that unfairly impact specific groups), privacy considerations, and security considerations.
- The conference expects that many papers will be foundational research and not tied to particular applications, let alone deployments. However, if there is a direct path to any negative applications, the authors should point it out. For example, it is legitimate to point out that an improvement in the quality of generative models could be used to generate deepfakes for disinformation. On the other hand, it is not needed to point out that a generic algorithm for optimizing neural networks could enable people to train models that generate Deepfakes faster.
- The authors should consider possible harms that could arise when the technology is being used as intended and functioning correctly, harms that could arise when the technology is being used as intended but gives incorrect results, and harms following from (intentional or unintentional) misuse of the technology.
- If there are negative societal impacts, the authors could also discuss possible mitigation strategies (e.g., gated release of models, providing defenses in addition to attacks, mechanisms for monitoring misuse, mechanisms to monitor how a system learns from feedback over time, improving the efficiency and accessibility of ML).

11. Safeguards

Question: Does the paper describe safeguards that have been put in place for responsible release of data or models that have a high risk for misuse (e.g., pretrained language models, image generators, or scraped datasets)?

Answer: [NA] N/A

Justification: Our paper does not involve the release of data or models that have a high risk for misuse. Therefore, this question is not applicable.

Guidelines:

- The answer NA means that the paper poses no such risks.
- Released models that have a high risk for misuse or dual-use should be released with necessary safeguards to allow for controlled use of the model, for example by requiring that users adhere to usage guidelines or restrictions to access the model or implementing safety filters.
- Datasets that have been scraped from the Internet could pose safety risks. The authors should describe how they avoided releasing unsafe images.
- We recognize that providing effective safeguards is challenging, and many papers do
 not require this, but we encourage authors to take this into account and make a best
 faith effort.

12. Licenses for existing assets

Question: Are the creators or original owners of assets (e.g., code, data, models), used in the paper, properly credited and are the license and terms of use explicitly mentioned and properly respected?

Answer: [Yes] Yes

Justification: We have properly credited the creators and original owners of the datasets and models used in our work. The licenses and terms of use are explicitly mentioned in Section 4 of our paper.

Guidelines:

- The answer NA means that the paper does not use existing assets.
- The authors should cite the original paper that produced the code package or dataset.
- The authors should state which version of the asset is used and, if possible, include a URL.
- The name of the license (e.g., CC-BY 4.0) should be included for each asset.
- For scraped data from a particular source (e.g., website), the copyright and terms of service of that source should be provided.
- If assets are released, the license, copyright information, and terms of use in the
 package should be provided. For popular datasets, paperswithcode.com/datasets
 has curated licenses for some datasets. Their licensing guide can help determine the
 license of a dataset.
- For existing datasets that are re-packaged, both the original license and the license of the derived asset (if it has changed) should be provided.
- If this information is not available online, the authors are encouraged to reach out to the asset's creators.

13. New Assets

Question: Are new assets introduced in the paper well documented and is the documentation provided alongside the assets?

Answer: [Yes] Yes

Justification: We have introduced new assets in the form of original code, and they are well documented. Detailed documentation is provided alongside the assets to ensure reproducibility and ease of use.

Guidelines:

- The answer NA means that the paper does not release new assets.
- Researchers should communicate the details of the dataset/code/model as part of their submissions via structured templates. This includes details about training, license, limitations, etc.
- The paper should discuss whether and how consent was obtained from people whose asset is used.
- At submission time, remember to anonymize your assets (if applicable). You can either create an anonymized URL or include an anonymized zip file.

14. Crowdsourcing and Research with Human Subjects

Question: For crowdsourcing experiments and research with human subjects, does the paper include the full text of instructions given to participants and screenshots, if applicable, as well as details about compensation (if any)?

Answer: [NA] N/A

Justification: Our paper does not involve crowdsourcing nor research with human subjects. Therefore, this question is not applicable.

- The answer NA means that the paper does not involve crowdsourcing nor research with human subjects.
- Including this information in the supplemental material is fine, but if the main contribution of the paper involves human subjects, then as much detail as possible should be included in the main paper.

 According to the NeurIPS Code of Ethics, workers involved in data collection, curation, or other labor should be paid at least the minimum wage in the country of the data collector.

15. Institutional Review Board (IRB) Approvals or Equivalent for Research with Human Subjects

Question: Does the paper describe potential risks incurred by study participants, whether such risks were disclosed to the subjects, and whether Institutional Review Board (IRB) approvals (or an equivalent approval/review based on the requirements of your country or institution) were obtained?

Answer: [NA] N/A

Justification: Our paper does not involve crowdsourcing nor research with human subjects. Therefore, this question is not applicable.

- The answer NA means that the paper does not involve crowdsourcing nor research with human subjects.
- Depending on the country in which research is conducted, IRB approval (or equivalent)
 may be required for any human subjects research. If you obtained IRB approval, you
 should clearly state this in the paper.
- We recognize that the procedures for this may vary significantly between institutions and locations, and we expect authors to adhere to the NeurIPS Code of Ethics and the guidelines for their institution.
- For initial submissions, do not include any information that would break anonymity (if applicable), such as the institution conducting the review.